

Modeling and Control of a Cable-Driven Series Elastic Actuator

Wulin Zou, Ningbo Yu

Abstract—Series elastic actuators (SEA) are playing an increasingly important role in the fields of physical human-robot interaction. This paper focuses on the modeling and control of a cable-driven SEA. First, the scheme of the cable-driven SEA has been proposed, and a velocity controlled DC motor has been used as its power source. Based on this, the model of the cable-driven SEA has been built up. Further, a two degrees of freedom (2-DOF) control approach has been employed to control the output torque. Simulation results have shown that the 2-DOF method has achieved better robust performance than the PD method.

I. INTRODUCTION

Series elastic actuator was first recommended by Pratt and Williamson for its benefits of greater shock tolerance, accurate and stable force output and the ability of energy storage [1]. Nowadays, SEAs are widely applied in various physical human-robot interaction applications, e.g., the SEA for walking robots [2], the compact rotary SEA for human assistive robots [3], the compact compliant actuator for rehabilitation robots [4], etc.

Cable actuation has attracted intensive research for its advantages of low inertia, flexible installation, remote actuation, etc. Cables with low weight to length ratio can change the force direction intentionally and easily, enable power transmission to a remote distance with less energy loss and space occupation [5], [6], and allow detachment of the actuation motor from the robot frame [7]. Besides, a cable actuated system can be a safe solution due to its unidirectional force constraint and property of breaking when the tension exceeding the threshold. Many cable actuated systems have been applied for physical human-robot interaction, such as the Lower extremity Powered ExoSkeleton (LOPES) [7], the Universal Haptic Drive (UHD) for upper extremity rehabilitation [8], the MR-compatible wrist robot [9], etc.

The force/torque controller of a series elastic actuator is designed to generate a spring deflection force/torque to follow a given command trajectory. Various control approaches have been developed for different SEAs to achieve high force/torque tracking performance. A Proportional-Integral-Differential (PID) control method was introduced in [10] to illustrate the concept and performance of a SEA explicitly. A lot of researchers have made important contributions to the development of SEA based on PID control [8], [9], [11]–[13]. Disturbance observer (DOB) based control methods

have been also adopted in [14]–[16] to enhance robustness. Wyeth proposed a cascaded torque control method with an inner velocity loop to overcome problems of non-linearities [11].

In this paper, the torque controller is designed using the 2-DOF method to track torque reference, eliminate disturbance and noise. Horowitz revealed that the 1-DOF configuration is unable to cope with the two problems of achieving a desired tracking response and attaining a good disturbance/noise rejection at the same time, but the 2-DOF controller could achieve these two goals simultaneously [17]. The reason is that the 2-DOF controller provides an independent way to design tracking response and optimize disturbance/noise rejection. Systematic introduction and design procedures about the 2-DOF control method can be found in [18], [19]. This paper is also an extensive work of [20]–[22].

This paper is organized as follows. Section II describes the concept and model of the velocity sourced cable-driven SEA. Details for the torque controller design are given in Section III. Simulations and results are presented in Section IV. Section V concludes the paper.

II. THE CABLE-DRIVEN SEA

A. The Model of the Cable-Driven SEA

The principle of a cable-driven SEA is shown in Fig. 1. A cable-spring series structure is introduced between the motor and the load. The power source of the actuator is supplied by a velocity controlled DC motor.

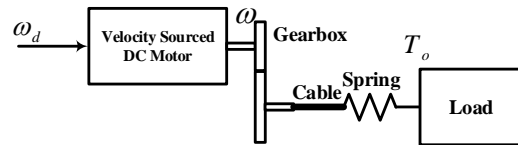


Fig. 1. The velocity sourced cable-driven SEA.

Neglecting the deflection of the cable, the velocity of the cable is given as

$$\omega_m = \frac{\omega}{K_g}. \quad (1)$$

Where, K_g is the gearbox ratio and ω is the output velocity of the DC motor. Then, the displacement of the cable is

$$\theta_m = \frac{\omega_m}{s}. \quad (2)$$

If the displacement of the load is θ_l , the spring deflection θ_s can be derived as

$$\theta_s = \theta_m - \theta_l. \quad (3)$$

Mr. Wulin Zou and Assoc. Prof. Dr. Ningbo Yu are with the Institute of Robotics and Automatic Information Systems, Nankai University, and Tianjin Key Laboratory of Intelligent Robotics, Nankai University, Haihe Education Park, Tianjin 300350, China.

E-mail: wlzou@mail.nankai.edu.cn, nyu@nankai.edu.cn

The torque T_o applied to the load is due to the deflection of the spring, such that

$$T_o = K_s \theta_s. \quad (4)$$

If the inertia and damping of the spring are considered, it becomes

$$T_o = (M_s s^2 + C_s s + K_s)(\theta_m - \theta_l). \quad (5)$$

Let $\theta_l = 0$ and combine (1), (2) and (5), there is

$$\frac{T_o(s)}{\omega(s)} = \frac{M_s s^2 + C_s s + K_s}{K_g s}. \quad (6)$$

B. Velocity Sourced DC Motor

To design a well performed SEA, a DC motor is used as the velocity source of the actuator. The reason that this idea is adopted is that velocity control is easier and more straightforward than current control. What's more, velocity control can overcome some undesirable effects caused by motor internal disturbance.

The schematic diagram of a velocity sourced DC motor is shown in Fig. 2. The velocity feedback regulated by a well tuned PI controller forms a stable closed loop so that the DC Motor system can track the reference signal quickly and accurately.

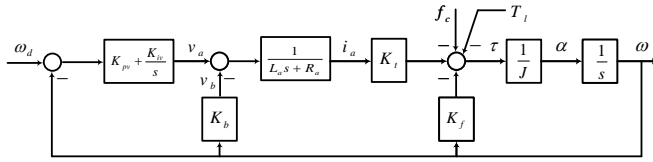


Fig. 2. The diagram of the velocity sourced DC motor.

When the current i_a flows through the motor coil, there is

$$L_a \frac{di_a}{dt} + i_a R_a + v_b = v_a. \quad (7)$$

Where v_a is the applied voltage across the motor terminals, R_a is the resistance of the motor winding, L_a is the inductance of the motor coil, and v_b is the back emf voltage that is linearly proportional to the angular velocity ω of the motor, such that $v_b = K_b \omega$.

The equation of the shaft rotating about a fixed axis is

$$K_t i_a - K_f \omega - f_c - T_l = J \alpha. \quad (8)$$

Where α is the angular acceleration such that $\alpha = \omega s$. The magnetic torque is linearly proportional (K_t) to the current i_a flowing through the motor coil. The viscous friction torque is in the opposite direction of the motion and is linearly proportional (K_f) to the angular velocity ω . f_c is the Coulomb friction and T_l is the load torque.

Substitute (7) into (8) and convert it to frequency domain equation, $\omega(s)$ can be obtained as

$$\omega(s) = \frac{v_a(s) K_t - (L_a s + R_a)(f_c(s) + T_l(s))}{J L_a s^2 + (J R_a + K_f L_a) s + K_f R_a + K_b K_t}. \quad (9)$$

C. Design of the Velocity Controller

In order to control the DC motor to be an effective velocity source, a PI controller is designed there. As shown in Fig. 2, the velocity controller has the form of

$$C_v(s) = K_{pv} + \frac{K_{iv}}{s}. \quad (10)$$

The velocity controller is tuned in the case of no load attached and neglecting the Coulomb friction, that is to say, the load torque T_l and the Coulomb friction f_c are set as zero. To create a system that will be of type 1, change (9) and (10) to the following form:

$$G_v(s) = \frac{\omega(s)}{v_a(s)} = \frac{\frac{K_t}{J L_a}}{(s + p_1)(s + p_2)}, \quad (11)$$

$$C_v(s) = \frac{K_{pv}(s + \frac{K_{iv}}{K_{pv}})}{s}. \quad (12)$$

Where $p_2 > p_1 > 0$ and both can be obtained from (9) and (11). Let

$$\frac{K_{iv}}{K_{pv}} = p_1, \quad (13)$$

then, the open loop transfer function becomes

$$\begin{aligned} H_{open} &= C_v(s) G_v(s) \\ &= \frac{K_{pv}(s + \frac{K_{iv}}{K_{pv}})}{s} \cdot \frac{\frac{K_t}{J L_a}}{(s + p_1)(s + p_2)} \\ &= \frac{K_{pv} K_t}{s(s + p_2)}. \end{aligned} \quad (14)$$

The closed loop transfer function will become a typical two order system, and has the form of

$$H_{closed} = \frac{\omega_n^2}{s^2 + 2\xi\omega_n s + \omega_n^2}. \quad (15)$$

According to (13), (14) and (15), there are

$$\begin{cases} K_{pv} = \frac{\omega_n^2 J L_a}{K_t} \\ K_{iv} = p_1 K_{pv} \\ 2\xi\omega_n = p_2 \end{cases}. \quad (16)$$

Given the desired performance of the closed loop system, the natural frequency ω_n and damping ratio ξ can be estimated. Then, the controller parameters can be obtained from (16). Further, the transfer function from the desired velocity input $\omega_d(s)$ to the actuator output torque $T_o(s)$ can be obtained by $P(s) = \frac{T_o(s)}{\omega_d(s)}$.

III. TORQUE CONTROLLER DESIGN

A. Controller with Optimal Transient

In this subsection, a possible way to design the best stabilizing controller and measure the quality will be introduced. Assume that $P(s)$ is strictly proper and denoted as the form of

$$P(s) = \frac{b(s)}{a(s)} = \frac{b_1 s^{n-1} + \dots + b_n}{a_0 s^n + a_1 s^{n-1} + \dots + a_n}. \quad (17)$$

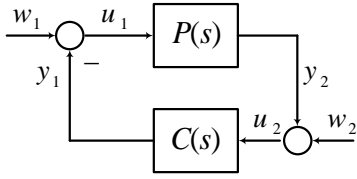


Fig. 3. Feedback system for stabilization.

Where $a(s)$ and $b(s)$ are coprime and $a_0 \neq 0$.

Consider the system shown in Fig. 3, if the closed loop system is internally stable and the external inputs $w_i(t), i = 1, 2$, are all impulse signals, all the internal signals $u_j(t), y_j(t), j = 1, 2$, will eventually settle to zero when time goes to infinity. So, the RMS value of $y_i(t), i = 1, 2$, when $w_i(t), i = 1, 2$, are unit impulses can be used to measure the quality of the performance as follow:

$$J = (\|y_1(t)\|_2^2 + \|y_2(t)\|_2^2) \Big|_{\substack{w_1(t)=\delta(t) \\ w_2(t)=0}} + (\|y_1(t)\|_2^2 + \|y_2(t)\|_2^2) \Big|_{\substack{w_1(t)=0 \\ w_2(t)=\delta(t)}}. \quad (18)$$

For different stabilizing controllers, their RMS value J are different. The minimum value of J denoted by J^* when $C(s)$ is chosen among all stabilizing controllers means that the best performance is achieved.

The transfer function from (w_1, w_2) to (y_1, y_2) is:

$$\begin{bmatrix} \frac{P(s)C(s)}{1 + P(s)C(s)} & \frac{C(s)}{1 + P(s)C(s)} \\ \frac{P(s)}{1 + P(s)C(s)} & \frac{-P(s)C(s)}{1 + P(s)C(s)} \end{bmatrix}. \quad (19)$$

The next problem to be solved is how to find the most optimal stabilizing controller. Firstly, there must exist a stable polynomial $d(s)$ called spectral factor of $a(-s)a(s) + b(-s)b(s)$ such that:

$$a(-s)a(s) + b(-s)b(s) = d(-s)d(s).$$

Now let $C(s) = \frac{q(s)}{p(s)}$ be the unique n -th order strictly proper pole placement controller such that:

$$a(s)p(s) + b(s)q(s) = d^2(s).$$

Then, this controller $C(s)$ is the most optimal controller which minimizes J and gives

$$J^* = \left\| \frac{d(s) - a(s)}{d(s)} \right\|_2^2 + \left\| \frac{b(s)}{d(s)} \right\|_2^2 + \left\| \frac{d(s) - p(s)}{d(s)} \right\|_2^2 + \left\| \frac{q(s)}{d(s)} \right\|_2^2. \quad (20)$$

If $w_i, i = 1, 2$, are external disturbances or noises, a stabilizing controller with optimal transient can eliminate them in a short time.

B. Stabilizing 2-DOF Controller

A closed loop system using 2-DOF controller to stabilize the plant $P(s)$ is shown in Fig. 4. The output z can track the reference input signal r in a satisfactory way, also, the disturbance d and the noise n can be eliminated close to zero in a short time.

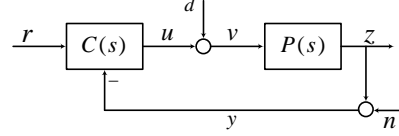


Fig. 4. The 2-DOF control configuration.

The stabilizing 2-DOF controller based on the controller with optimal transient is shown in Fig. 5. Let $C_0(s)$ be a stabilizing controller with optimal transient: $C_0(s) = \frac{q(s)}{p(s)}$. Let $M(s), N(s), X(s), Y(s)$ be:

$$\begin{aligned} M(s) &= \frac{a(s)}{d(s)}, N(s) = \frac{b(s)}{d(s)}, \\ X(s) &= \frac{p(s)}{d(s)}, Y(s) = \frac{q(s)}{d(s)}. \end{aligned} \quad (21)$$

Then $M(s), N(s), X(s), Y(s)$ are all stable transfer functions satisfying:

$$\begin{aligned} P(s) &= \frac{N(s)}{M(s)}, C_0(s) = \frac{Y(s)}{X(s)}, \\ M(s)X(s) + N(s)Y(s) &= 1. \end{aligned}$$

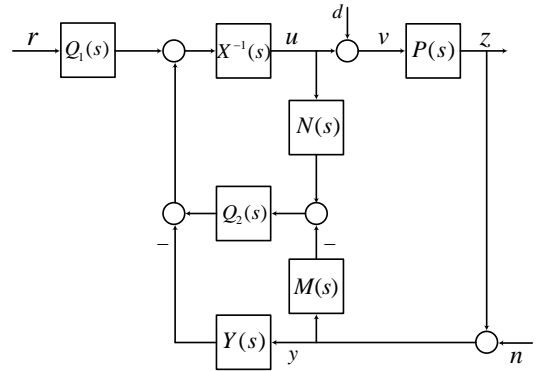


Fig. 5. Stabilizing 2-DOF control structure.

Denote the set of all the 2-DOF controllers which give stable closed loop systems by $\Omega(P)$:

$$\Omega(P) = \left\{ C(s) = \left[\begin{array}{cc} \frac{Q_1(s)}{X(s) - N(s)Q_2(s)} & \frac{Y(s) + M(s)Q_2(s)}{X(s) - N(s)Q_2(s)} \end{array} \right] \right\}. \quad (22)$$

Where, $Q_1(s), Q_2(s)$ are arbitrary stable transfer functions.

Every stabilizing 2-DOF controller has the form shown in Fig. 5. For a fixed plant $P(s)$, if we plug a stabilizing 2-DOF controller of this form to a closed loop transfer function, then the closed loop transfer function becomes a function of $Q_1(s)$ and $Q_2(s)$. The problem becomes choosing good

$Q_1(s)$ and $Q_2(s)$ to meet the design specifications, as long as they are stable.

The four transfer functions from r to the internal variables u, v, y, z depend only on $Q_1(s)$:

$$\begin{bmatrix} \frac{C_1(s)}{1 + P(s)C_2(s)} \\ \frac{C_1(s)}{1 + P(s)C_2(s)} \\ \frac{P(s)C_1(s)}{1 + P(s)C_2(s)} \\ \frac{P(s)C_1(s)}{1 + P(s)C_2(s)} \end{bmatrix} = \begin{bmatrix} M(s) \\ M(s) \\ N(s) \\ N(s) \end{bmatrix} Q_1(s). \quad (23)$$

The eight transfer functions from d, n to u, v, y, z depend only on $Q_2(s)$:

$$\begin{bmatrix} \frac{-P(s)C_2(s)}{1 + P(s)C_2(s)} & \frac{-C_2(s)}{1 + P(s)C_2(s)} \\ \frac{1}{1 + P(s)C_2(s)} & \frac{-C_2(s)}{1 + P(s)C_2(s)} \\ \frac{P(s)}{1 + P(s)C_2(s)} & \frac{1}{1 + P(s)C_2(s)} \\ \frac{P(s)}{1 + P(s)C_2(s)} & \frac{-P(s)C_2(s)}{1 + P(s)C_2(s)} \end{bmatrix} = \begin{bmatrix} -N(s)Y(s) & -M(s)Y(s) \\ M(s)X(s) & -M(s)Y(s) \\ N(s)X(s) & M(s)Y(s) \\ N(s)X(s) & -N(s)X(s) \end{bmatrix} \cdot \begin{bmatrix} M(s) \\ M(s) \\ N(s) \\ N(s) \end{bmatrix} Q_2(s) \begin{bmatrix} N(s) & M(s) \end{bmatrix}. \quad (24)$$

This makes choosing $Q_1(s)$ and choosing $Q_2(s)$ decoupled and rather convenient.

C. Parameterization of $Q_1(s)$ and $Q_2(s)$

Since the transfer function from the reference input r to the output signal z is $N(s)Q_1(s)$, let

$$Q_1(s) = \frac{\bar{\omega}_n^2}{N(s)(s^2 + 2\bar{\xi}\bar{\omega}_n s + \bar{\omega}_n^2)}.$$

Then, the transfer function from r to z becomes

$$N(s)Q_1(s) = \frac{\bar{\omega}_n^2}{s^2 + 2\bar{\xi}\bar{\omega}_n s + \bar{\omega}_n^2}.$$

Considering that $Q_2(s)$ is mainly used to filter the disturbance d and noise n whose industrial frequencies are assumed to be 50 Hz, let

$$Q_2(s) = \frac{1}{s/(100\pi) + 1}.$$

IV. SIMULATIONS AND RESULTS

The cable-driven SEA parameters are listed in Table I.

TABLE I
PARAMETERS OF THE CABLE-DRIVEN SEA.

J	$6.96 \times 10^{-6} \text{kg} \cdot \text{m}^2$
L_a	0.62mH
R_a	2.07 Ω
K_t	0.0525Nm/A
K_b	0.0525Vs/rad
K_f	0.00001Nm/(rad/s)
K_s	138Nm/rad
K_g	156 : 1
C_s	0.01Nm/(rad/s)
J_t	0.1kg · m ²
M_s	0.00001kg · m ²

A. Simulation Results of the Velocity Control

The transfer function from $v_a(s)$ to $\omega(s)$ is:

$$\frac{v_a(s)}{\omega(s)} = \frac{1.217e07}{s^2 + 3340s + 6.435e05}.$$

When the damping ratio ξ is chosen to be 0.88, the coefficients of the proportional-integral controller are $K_{pv} = 0.26$, $K_{iv} = 53.5$. The step response of velocity closed loop system is shown in Fig. 6. The rise time of the velocity closed loop system is within 0.002s, almost no overshoot, can meet the requirements of a velocity source.

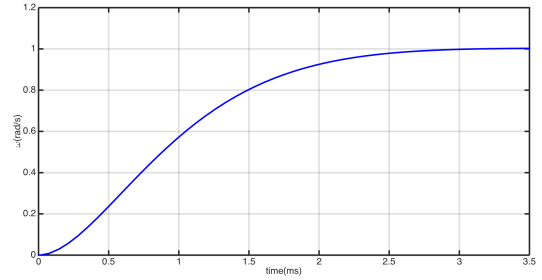


Fig. 6. Step response of the velocity control

B. Simulation Results of the Torque Control

The transfer function $P(s)$ from $\omega_d(s)$ to $T_o(s)$ when the load is fixed is:

$$P(s) = \frac{0.2034s^3 + 245.1s^2 + 2.848e06s + 5.761e08}{s^4 + 3340s^3 + 3.817e06s^2 + 6.54e08s}$$

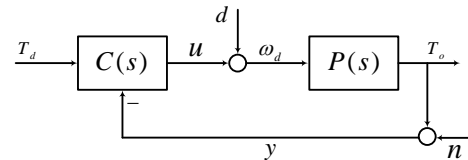


Fig. 7. Torque control structure for the cable-driven SEA.

The stabilizing 2-DOF controller can be obtained by choosing $\bar{\omega}_n = 451.24$ and $\bar{\xi} = 0.826$. In the simulation, a PD controller $C_{PD}(s) = 490 + 0.1s$ is used for comparison. The torque control structure for the cable-driven SEA is shown in Fig. 7.

In the first simulation, the disturbance d and the noise n are set to zero. Then, the step responses from $T_d(s)$ to $T_o(s)$ of the two control method are shown in Fig. 8. Both the two method tracks the step input quickly and accurately.

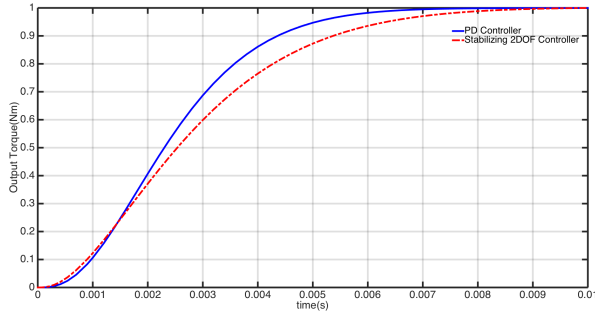


Fig. 8. Tracking step signal without disturbance and noise

In the second simulation, the disturbance d and the noise n are set as gaussian white noises with zero mean. The input signal T_d is set as a sinusoidal signal with frequency of 5 Hz and amplitude of 1 Nm. The tracking results are shown in Fig. 9. It is clear that the stabilizing 2-DOF controller can enhance the system robustness.

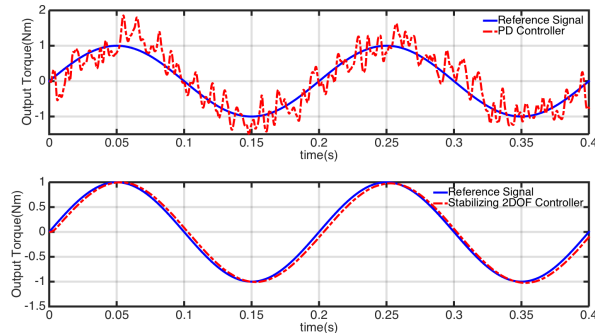


Fig. 9. Tracking sinusoidal signal with disturbance and noise

V. CONCLUSIONS

This paper demonstrates the efficacy of the 2-DOF control approach for the challenging torque control problem of a cable-driven SEA. The 2-DOF torque controller performed better compared with the PD method in the presence of noise and disturbance in the simulations. The torque control performance can be conveniently adjusted by choosing appropriate filter $Q_1(s)$ and $Q_2(s)$.

Further research will be focused on the impedance control of the cable-driven SEA.

REFERENCES

- [1] G. A. Pratt and M. M. Williamson, "Series elastic actuators," in *Proceedings of the IEEE/RSJ International Conference on Intelligent Robots and Systems*, vol. 1, 1995, Conference Proceedings, pp. 399–406.
- [2] D. W. Robinson, J. E. Pratt, D. J. Paluska, and G. Pratt, "Series elastic actuator development for a biomimetic walking robot," in *Proceedings of the IEEE/ASME International Conference on Advanced Intelligent Mechatronics*, 1999, Conference Proceedings, pp. 561–568.

- [3] K. Kong, J. Bae, and M. Tomizuka, "A compact rotary series elastic actuator for human assistive systems," *IEEE/ASME Transactions on Mechatronics*, vol. 17, no. 2, pp. 288–297, 2012.
- [4] H. Yu, S. Huang, N. V. Thakor, G. Chen, S. L. Toh, M. S. Cruz, Y. Ghorbel, and C. Zhu, "A novel compact compliant actuator design for rehabilitation robots," in *Proceedings of the IEEE International Conference on Rehabilitation Robotics*, 2013, Conference Proceedings, pp. 1–6.
- [5] D. Chapuis, R. Gassert, G. Ganesh, E. Burdet, and H. Bleuler, "Investigation of a cable transmission for the actuation of MR compatible haptic interfaces," in *Proceedings of the First IEEE/RAS-EMBS International Conference on Biomedical Robotics and Biomechanics*, 2006, Conference Proceedings, pp. 426–431.
- [6] R. J. Caverly, J. R. Forbes, and D. Mohammadshahi, "Dynamic modeling and passivity-based control of a single degree of freedom cable-actuated system," *IEEE Transactions on Control Systems Technology*, vol. 23, no. 3, pp. 898–909, 2015.
- [7] J. F. Veneman, R. Ekkelenkamp, R. Kruidhof, F. C. V. D. Helm, and H. V. D. Kooij, "A series elastic-and bowden-cable-based actuation system for use as torque actuator in exoskeleton-type robots," *The International Journal of Robotics Research*, vol. 25, no. 3, pp. 261–281, 2006.
- [8] J. Oblak, I. Cikajlo, and Z. Matjačić, "Universal haptic drive: A robot for arm and wrist rehabilitation," *IEEE Transactions on Neural Systems and Rehabilitation Engineering*, vol. 18, no. 3, pp. 293–302, 2010.
- [9] F. Sergi and M. K. O'Malley, "On the stability and accuracy of high stiffness rendering in non-backdrivable actuators through series elasticity," *Mechatronics*, vol. 26, pp. 64–75, 2015.
- [10] D. W. Robinson, "Design and analysis of series elasticity in closed-loop actuator force control," Thesis, Massachusetts Institute of Technology, 2000.
- [11] G. Wyeth, "Control issues for velocity sourced series elastic actuators," in *Proceedings of the Australasian Conference on Robotics and Automation*, 2006, Conference Proceedings.
- [12] H. Vallery, R. Ekkelenkamp, H. V. D. Kooij, and M. Buss, "Passive and accurate torque control of series elastic actuators," in *Proceedings of the IEEE/RSJ International Conference on Intelligent Robots and Systems*, 2007, Conference Proceedings, pp. 3534–3538.
- [13] D. Accoto, G. Carpino, F. Sergi, N. L. Tagliamonte, L. Zollo, and E. Guglielmelli, "Design and characterization of a novel high-power series elastic actuator for a lower limb robotic orthosis," *International Journal of Advanced Robotic System*, vol. 10, p. 359, 2013.
- [14] K. Kong, J. Bae, and M. Tomizuka, "Control of rotary series elastic actuator for ideal force-mode actuation in human-robot interaction applications," *IEEE/ASME Transactions on Mechatronics*, vol. 14, no. 1, pp. 105–118, 2009.
- [15] S. Yoo and W. K. Chung, "SEA force/torque servo control with model-based robust motion control and link-side motion feedback," in *Proceedings of the IEEE International Conference on Robotics and Automation*, 2015, Conference Proceedings, pp. 1042–1048.
- [16] J. Lu, K. Haninger, W. Chen, and M. Tomizuka, "Design and torque-mode control of a cable-driven rotary series elastic actuator for subject-robot interaction," in *Proceedings of the IEEE International Conference on Advanced Intelligent Mechatronics*, 2015, Conference Proceedings, pp. 158–164.
- [17] I. M. Horowitz, *Synthesis of feedback systems*. London: Academic Press, 1963.
- [18] L. Qiu and K. Zhou, *Introduction to feedback control*. New Jersey: Pearson Prentice Hall, 2010.
- [19] P. Huang, "Theoretical and experimental studies on two-degree-of-freedom controllers," Thesis, Hong Kong University of Science and Technology, 2015.
- [20] W. Zou, W. Tan, Z. Yang, and N. Yu, "Torque control of a cable-driven series elastic actuator using the 2-DOF method," in *Proceedings of the Chinese Control Conference*, 2016, Conference Proceedings, pp. 6239–6243.
- [21] W. Zou, Z. Yang, W. Tan, M. Wang, J. Liu, and N. Yu, "Impedance control of a cable-driven series elastic actuator with the 2-DOF control structure," in *Proceedings of the IEEE/RSJ International Conference on Intelligent Robots and Systems*, 2016, Conference Proceedings, pp. 3347–3352.
- [22] W. Zou, W. Tan, Z. Yang, and N. Yu, "Augmented virtual stiffness rendering of a cable-driven SEA for human-robot interaction," *The IEEE/CAA Journal of Automatica Sinica*, 2017.